The Interaction of Water with the Oxygen-Terminated, Polar Surface of ZnO

M. Kunat, St. Gil Girol, U. Burghaus,† and Ch. Wöll*

Physikalische Chemie I, Ruhr-Universität Bochum, 44801 Bochum, Germany

Received: May 30, 2003; In Final Form: September 5, 2003

The adsorption of H_2O on the oxygen-terminated polar surface of ZnO, ZnO(000-1), has been studied by He atom scattering (HAS), low-energy electron diffraction (LEED), adsorption probability measurements, He atom reflectivity measurements as a function of exposure and surface temperature (He atom thermal desorption measurements, "He-TDS"), and X-ray photoelectron spectroscopy (XPS). The clean O−ZnO(000-1) surface is characterized by an ordered (1×3) oxygen vacancy structure which converts to a (1×1) hydrogen (OH)-terminated structure upon dissociative H_2O adsorption, even at adsorption temperatures as low as $T_S = 200$ K. The formation of the OH-species is accompanied by the formation of a shoulder in the XPS O 1s line. A detailed investigation of the coverage dependence of the H_2O adsorption probability indicates the presence of a distinct precursor state. The initial trapping probability is $S_0 = 0.8 \pm 0.1$. The most probable microscopic adsorption mechanism which is consistent with the obtained data is a trapping of the molecules in a precursor state and a subsequent dissociation at O vacancy sites, yielding two OH-species per dissociated H_2O molecule on the surface. The binding energy of the OH-species amounts to ∼130 kJ/mol as determined from He-TDS curves.

1. Introduction

Metal oxides are used for many different applications, e.g., as components of biocompatible implants[1] and as photocatalysts for hydrogen production from water.[2] In particular, zinc oxide plays a vital role in chemistry, material science, and modern technology.[3−5] ZnO-based heterogeneous catalysts are, for example, used for methanol synthesis, olefin hydrogenation, and gas-sensor applications. Presently, the most prominent application of ZnO is industrial methanol synthesis. For the low-temperature synthesis of methanol from syn-gas (a mixture of CO_2, CO, and hydrogen), which takes place at a total pressure of 50−100 bar and at reaction temperatures in the range of 493−573 K,[6] a powder containing Cu, ZnO, and Al_2O_3 is used (see, e.g., refs 6,7).

The present study on the interaction of water with the O−ZnO surfaces is a part of a longer term project to study the interaction of small molecules with ZnO surfaces (see refs 8−10 for CO and H_2 adsorption on polar surfaces of ZnO, ref 11 for a study about the clean Al_2O_3 $(11\bar{2}0)$ surface, ref 12 for CO and hydrogen coadsorption measurements on Zn−ZnO, and, e.g., ref 13 for a Monte Carlo modeling of the corresponding adsorption probability measurements).

2. Brief Survey of the Literature

A number of results from previous studies, which are of importance for the discussion of the presented data, will be briefly summarized before presenting the new results.

Whereas the adsorption of water on metal surfaces has been studied extensively (see ref 14 and the references therein), there are fairly few papers on the adsorption of water on metal oxide surfaces such as ZnO (see refs 15−22, 23), sapphire (see, e.g., ref 24), TiO_2 (see, e.g., refs 25, 26), MgO (see, e.g., refs 27, 28), and NiO (see, e.g., ref 29). For the case of ZnO single crystal surfaces, we are aware of only two previous experimental investigations.[22,23] In a TDS and UPS study of Zwicker and Jacobi,[22] the adsorption and condensation of H_2O on polar and nonpolar surfaces of ZnO has been thoroughly investigated. In these previous experiments the ZnO crystals have been doped with Zn or In to enhance their electrical conductance and (1×1) LEED patterns have been observed for all surfaces prior to the adsorption measurements. Upon adsorption of H_2O at 100 K, no ordered overlayer structure could be observed by LEED; from the TDS and UPS results an associative adsorption has been deduced, and no indication of dissociation was observed. The TDS curves of H_2O/O−ZnO were dominated (in the monolayer coverage range) by a sharp peak at ∼200 K and a broad structure in the temperature range of 250−500 K. The results reported by Zwicker and Jacobi[22] were essentially confirmed by a later study by Zhang et al.,[23] where in a TDS study a multilayer desorption peak at 155 K and a second sharp desorption peak at 195 K were reported. For ZnO powders, on the other hand, Sengupta et al.[18] have proposed dissociative adsorption of H_2O on the basis of ESR and conductivity measurements. Heating of the powders was found to result in the desorption of H_2 and OH radicals.[18]

In previous theoretical work based on DFT calculations, a stabilization of the polar ZnO surfaces by a charge transfer from the O- to the Zn-terminated side of a polar surface has been proposed (see ref 30). These conclusions were, however, questioned by another theoretical study, where the (1×1)-surface was found to be instable if larger unit-cells were considered.[31,32] The possibility of surface stabilization by adsorbates has also been considered, but no effect was found for the case of dissociative H_2O adsorption (see ref 21). It has to be noted, however, that the theoretical studies of Wander et al.[21,30] were based on models assuming a (1×1) structure for the clean surface; in more recent studies also larger unit cells were considered.[31,32] In cluster calculations reported by Martins

* Corresponding author. E-mail: woell@pc.ruhr-uni-bochum.de.
† New address: Department of Chemistry, North Dakota State University, Fargo, ND.

10.1021/jp030675z CCC: $25.00
Published on Web 11/27/2003

et al.[20] both molecular and dissociative adsorption of H_2O on O−ZnO surfaces were considered and, for molecular H_2O, a strong interaction with Zn sites was found. In another theoretical study by Casarin et al.,[17] only associative adsorption of H_2O on ZnO(0001)-clusters was considered. Interestingly, dissociation of H_2O has been predicted theoretically to occur on the nonpolar surface of ZnO (see refs 15, 17).

The morphology of ZnO surfaces has been studied by scanning tunneling microscopy (see, e.g., ref 33); however, no STM study on the adsorption of H_2O on ZnO surfaces has been conducted so far.

Recently, a number of works have appeared on the interaction of water with a similar metal oxide system, namely the rutile TiO_2(110) surface. Although older studies assumed molecular H_2O adsorption on TiO_2(110), a combined experimental (STM) and theoretical (DFT) study of Schaub et al.[25] has provided convincing evidence that oxygen vacancies in the surface layer can act as active sites for H_2O dissociation, producing two hydroxyl-species per dissociated water molecule. This conclusion is consistent with another STM study on H_2O/TiO_2(110) by Brookes et al.,[34] where also defect sites have been proposed to be responsible for the dissociation process.

With regard to the structure of the clean O−ZnO surface, recently it was found that the clean (hydrogen-free)-surface exhibits a (1 × 3) reconstruction. Upon exposure to atomic hydrogen the surface reconstruction is removed, leading to the formation of a H(1 × 1)-overlayer,[35] similar to the situation for the Zn-terminated polar Zn−ZnO(0001) surface.[9]

3. Experimental Procedures

The measurements have been conducted using two different apparatuses, namely, a molecular beam system equipped with XPS and LEED[36] and a modified Leybold XPS spectrometer equipped with an EA11 hemispherical energy analyzer, a standard X-ray source and a monochromatic X-ray source (Al Kα with $h\nu = 1486.6$ eV). The source for the supersonic molecular beam is attached to a scattering chamber and to a differentially pumped drift tube. At the end of the drift tube a magnetic mass filter for the detection of the scattered He atoms is mounted. Whereas the total scattering angle is fixed, different incidence, α_i, and scattering angles can be accessed by rotating the sample. The scattering chamber contains a second mass spectrometer (used for the King and Wells[37] adsorption probability measurements), LEED, XPS (with Al Kα radiation), and a differentially pumped sputter gun.

The surface has been exposed to water either by backfilling the UHV-chamber using a leak valve or by dosing water through a capillary that ended approximately 5 cm in front of the ZnO-substrate. By comparing the amounts of water adsorbed on the surface using the two different methods we could determine the factor by which the effective pressure in front of the ZnO-surface for the capillary is higher than the reading of the pressure gauge; this factor amounts to 10. All exposures given in the following have been corrected for this factor when the dosing was carried out using the capillary.

As a third method to expose the O−ZnO surface to water, a molecular beam with H_2O seeded in He has been used which directly impinges on the O−ZnO surface (beam diameter at the position of the sample ∼3 mm). The seeded beam was produced by passing a stream of He gas through a washing bottle (cf., ref 26) containing high purity H_2O. The resulting gas mixture (total pressure ∼ 10 bar) has then been expanded through a room-temperature nozzle with a diameter of 20 μm. The washing bottle and the gas lines have been kept at a temperature of approximately 380 K. We estimate the H_2O flux to 0.002 ML/s from the results of the adsorption probability measurements and by assuming a saturation coverage of 1 ML (= 1.092×10^{15} particles/cm^2) at 200 K (see part 4 for details). The kinetic energy, E_i, of H_2O (seeded in He) can be determined by measuring the velocity of specularly scattered He atoms (using a time-of-flight technique (TOF)) and assuming that the velocity of the He atoms and that of the H_2O molecules are the same. The corresponding measurements yield a value of $E_i(H_2O) = 0.2$ eV (E_i(He) = 0.05 eV). The mass filter mounted at the end of the drift tube is optimized for the detection of He atoms and cannot be used for the detection of H_2O.

The ZnO single crystals (purchased from MaTeck crystals) were cleaned by a procedure consisting of cycles of Ar^+ sputtering (800 V, ∼1 μA, 4 h, $T_s = 650$ K) followed by annealing in oxygen (1×10^{-6} Torr, $T_s \sim 850$ K, 2 min) and in UHV ($T_s = 850$ K, 5 min) as already applied in previous investigations.[8] Typically, about two sputtering cycles with annealing of the crystal in UHV were followed by one cycle with annealing in an oxygen ambient. After a few preparation cycles, a pronounced LEED pattern and a distinct specular He peak revealed the presence of a structurally well-defined surface. From the fact that no C 1s signal was seen in the XP spectra we estimate that the contamination levels for carbon-containing species are less than 0.05 ML. The measurements have been conducted with two different samples (in each apparatus) of the O-terminated ZnO(000-1) surface. The results for the two different specimens did not reveal significant differences. Therefore data corresponding to the different samples have not explicitly been distinguished in the presented figures.

All gases employed were of research purity (99.9999% for He and 99.99% for CO); the H_2O used for backfilling the UHV-chamber was additionally cleaned by pump−freeze−thaw cycles. The ZnO single crystal could be cooled to a temperature, T_s, of approximately 70 K by using liquid helium. The thermocouple which was clamped to the side of the crystal has been calibrated by thermal desorption measurements (heating rate of 1 K/s) of *n*-butane multilayers (maximum of multilayer TDS signal at $T_m = 111$ K), in agreement with, e.g., ref 38. The base pressure of the UHV-chamber amounted to a 1×10^{-10} mbar, with a partial pressure of H_2O below 1×10^{-11} mbar.

4. Presentation of the Results

(a) LEED and He Atom Scattering Results. Figure 1 shows a set of He atom angular distributions recorded for O−ZnO surfaces exposed to different amounts of water. The data in Figure 1A reveal the (1 × 3) diffraction pattern typical for the clean, hydrogen-free O−ZnO surface. Exposing the surface to a very small (0.19 L; 1 L = 1×10^{-6} Torr·s) amount of H_2O (by dosing through the capillary) at $T_s = 150$ K results in a strong suppression of the diffraction peaks, which is accompanied by the formation of a pronounced cosine-shaped background in the He atom angular distributions (Figure 1B). Figures 1C and 1D show He atom angular distributions which were obtained after heating the surface to 190 K (370 K). These data reveal a distinctly different (1 × 1) diffraction pattern where the third-order peaks seen for the clean, hydrogen-free surface are absent. This (1 × 1) diffraction pattern is virtually identical to that recorded for the O−ZnO surface exposed to atomic hydrogen.[35]

LEED patterns corresponding to the He atom angular distributions are shown in Figure 2. The first row (Figure 2A)

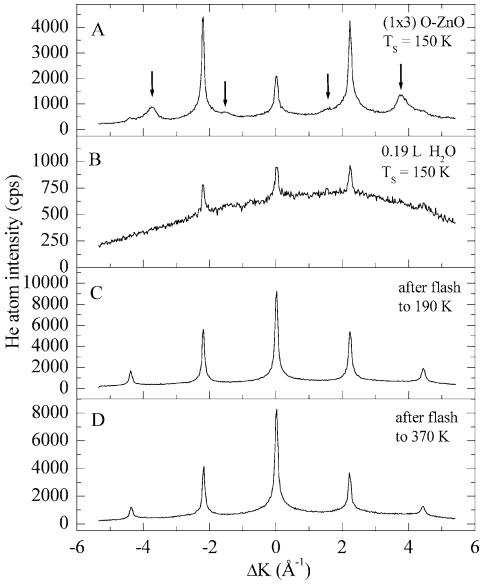

Figure 1. He atom angular distributions recorded for the O−ZnO surface. (A**)** (1 × 3) structure observed for the clean surface; (B) (1 × 1) structure obtained after exposure to H_2O; (C) and (D) angular distributions measured after flashing the surface to different temperatures. (Measuring parameters as indicated.)

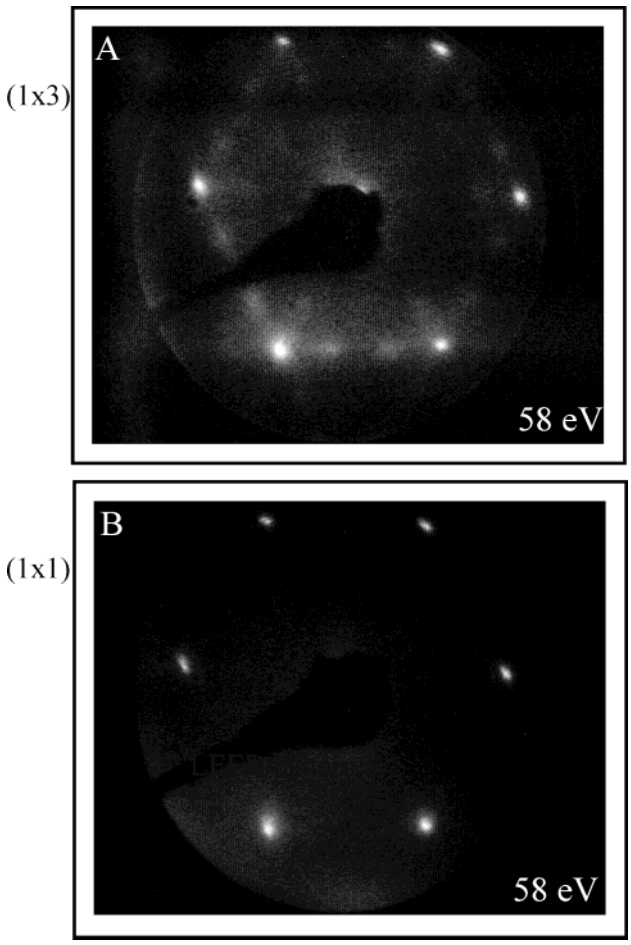

Figure 2. LEED pattern of (***A***) the (1 × 3) structure of the clean O−ZnO surface and (B) of the (1 × 1) structure of the surface obtained after saturating with H_2O.

shows the LEED pattern obtained from the clean surface. After saturating the surface with H_2O (in the temperature range of 200−400 K) the LEED patterns shown in the lower panel (Figure 2B) have been detected.

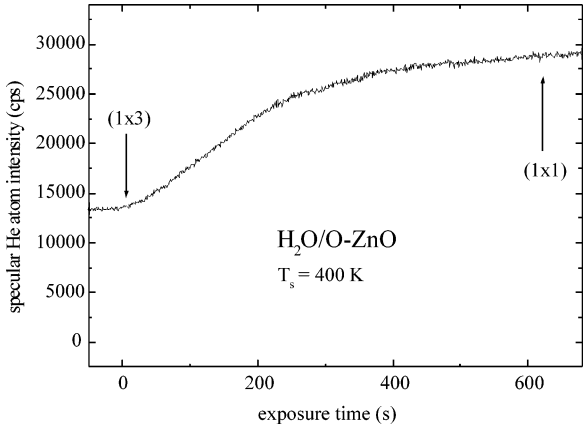

Figure 3. Reflectivity of the O−ZnO surface for He atoms while exposing to H_2O by backfilling the scattering chamber at 4 × 10^{-9} mbar (measuring parameters as indicated).

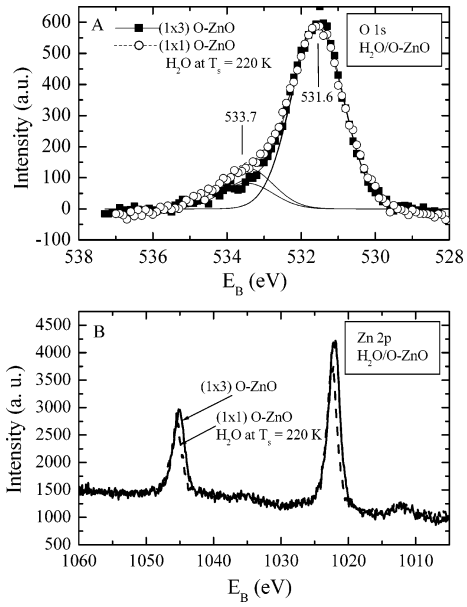

Figure 4. XPS data recorded for the clean (solid lines) and the H_2O saturated surface (dashed lines) in the (A) O 1s and (B) the Zn 2p binding energy range, respectively, as obtained at grazing exit angles of the photoelectrons.

In Figure 3 we present the intensity of the specularly reflected He beam, I_{He}, as a function of exposure to H_2O (carried out by backfilling the chamber to a pressure of 4 × 10^{-9} mbar) at a surface temperature of 400 K. The specular intensity increases significantly upon exposure to water and reaches a constant value after approximately 600 s (which equals a total exposure of 2.4 L). He atom angular distributions recorded after this exposure are indistinguishable from the one shown in Figure 1C, the LEED pattern corresponds to that shown in Figure 2B.

(b) X-ray Photoelectron Spectroscopy. In Figure 4 we display O 1s and Zn 2p XP spectra recorded for the clean O−ZnO(000-1) surface as well as for the same surface saturated with H_2O at 220 K. The XP spectra have been measured at grazing exit angles (75° ± 5°) of the photoelectrons in order to enhance the surface sensitivity. Exposure of the O−ZnO surface to H_2O is found to lead to the formation of a weak, distinct shoulder on the high-energy side of the O 1s line (see the fit in Figure 4A and the discussion below). XP spectra virtually identical to that shown in Figure 4 for the H_2O-saturated surface at 220 K have been obtained after exposure to hydrogen atoms,

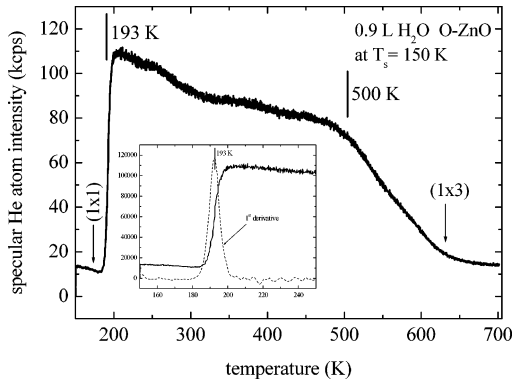

Figure 5. He atom reflectivity curves recorded after exposure of the O−ZnO surface to H_2O at 150 K while increasing the surface temperature (solid line). ("He-TDS" method). The inset shows an enlarged view of the temperature regime between 150 and 250 K together with the first derivative of the reflectivity curve.

see ref 9 for details. Note, that the Zn 2p XP lines for the clean surface are somewhat wider than for the H_2O-covered surfaces (Figure 4B).

(c) "He-TDS Measurements" (adsorption kinetics). To obtain kinetic data about water desorption and adsorption, the specular He atom intensity has been monitored while increasing the surface temperature ("He-TDS" method see, e.g., refs 39, 40) after saturating the surface with H_2O at 150 K (see Figure 5). The initial state of the surface (i.e., before water exposure) is characterized by the He atom angular distribution shown in Figure 1A; the peaks related to the (1×3)-structure are marked by arrows. The I_{He} vs T_s curve first shows a sharp increase at 193 K (see inset in Figure 5) and a broader structure with an edge at approximately 500 K, as indicated by the short lines in Figure 5.

(d) H_2O Adsorption Probability Measurements. The H_2O adsorption probability has been measured using the King and Wells method[37] and, simultaneously, by recording I_{He} vs exposure curves. For these experiments, a molecular beam with H_2O seeded in He has been directed on the ZnO surface (see above for experimental details).

A typical result is shown in Figure 6A, where we display the partial pressure of H_2O in the scattering chamber (left-hand scale, determined with the mass-spectrometer mounted in the scattering chamber) as a function of exposure time (the He/H_2O beam has been opened at $t = 0$ s). The vertical scale thus corresponds directly to $1 - S$ (see right-hand scale). The solid lines indicate the background and the saturation level, respectively. The intensity of the He atoms in the seeded beam reflected in the specular direction was measured simultaneously; a typical result is shown in Figure 6B. The saturation coverage of the surface with respect to the dissociative adsorption of water is determined from the sharp decrease of the sticking coefficient as shown in Figure 6A. Integration of the uptake curves (as shown in Figure 6A) then yield the coverage dependence of the adsorption probability of H_2O, $S(\Theta)$, as shown in Figure 6C (left-hand scale). The data clearly reveal that the adsorption probability is constant up to coverages of 0.9 ML, where it drops to zero, as expected.

The corresponding I_{He} vs coverage curves are shown in Figure 6C (right-hand scale). At $t = 0$, the counting rate amounts to about 300 Hz, which increases to 500−900 Hz in the course of the H_2O adsorption.

In Figure 7 we have compiled the results of a different set of experiments, where the dependence of $S(\Theta)$ on the surface temperature has been determined for a different geometry,

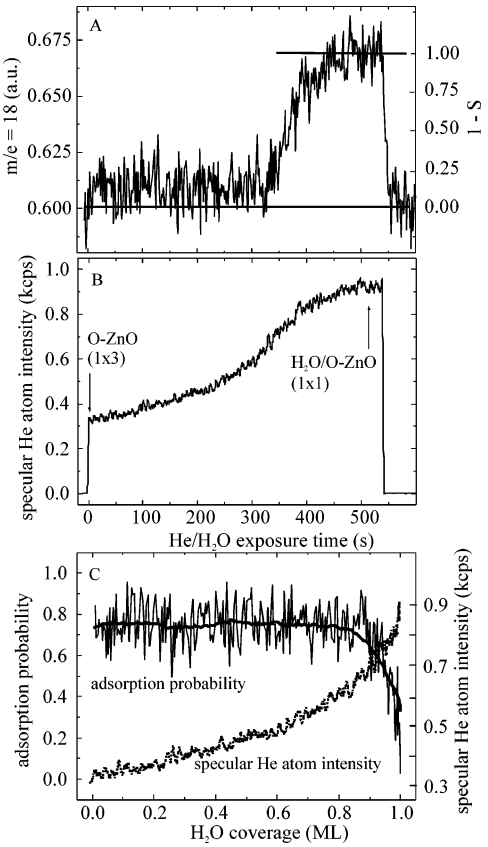

Figure 6. Typical example of H_2O uptake and He atom reflectivity curves, respectively, for O−ZnO as measured simultaneously using a He/H_2O-seeded molecular beam. (A) Partial H_2O pressure in the scattering chamber and (B) specular He atom intensity as a function of exposure time. (C) Integration of the curves shown in A and B. ($T_s = 250$ K; $T_N = 300$ K; $\alpha_i = 45.5°$; $E_i(H_2O) = 0.2$ eV; $E_i(He) = 0.05$ eV).

namely, for normal incidence of the H_2O molecules, again using the King and Wells method. The general shape of $S(\Theta)$ does not show a pronounced variation in the temperature range of 200−450 K except for the decrease in the saturation coverage which has been normalized with respect to $S(\Theta_{Sat}) = 1.0$ at $T_s = 200$ K. In that temperature range, $S(\Theta)$ remains approximately constant up to saturation of the surface where $S(\Theta)$ drops to zero, as expected. Above $T_s = 450$ K, the data shown in Figure 7 reveal a distinct change in the shape of $S(\Theta)$. At these higher substrate temperatures, instead of being constant $S(\Theta)$ shows a linear decrease before dropping to zero when the surface is saturated. In addition to these changes in the overall shape of the $S(\Theta)$-curves for larger substrate temperatures, a decrease of the absolute value of S_0 is observed. Figure 7B and Figure 7C show a compilation of the temperature dependence of S_0 and of Θ_{SAT}, respectively.

5. Discussion

(a) Structure of the Clean and the Adsorbate-Covered Surface. Both the He atom angular distributions (see Figure 1A) as well as the LEED pattern (see Figure 2A) reveal the presence of a (1×3) reconstruction of the clean O−ZnO surface, as reported in previous work.[35] When analyzing the pattern in detail it has to be considered that symmetry requires the presence of 3 different (1×3) domains rotated by 120° with respect to each other. The most important question with regard to the chemical activity of this surface is that about the microscopic structure of the reconstructed surface. In principle,

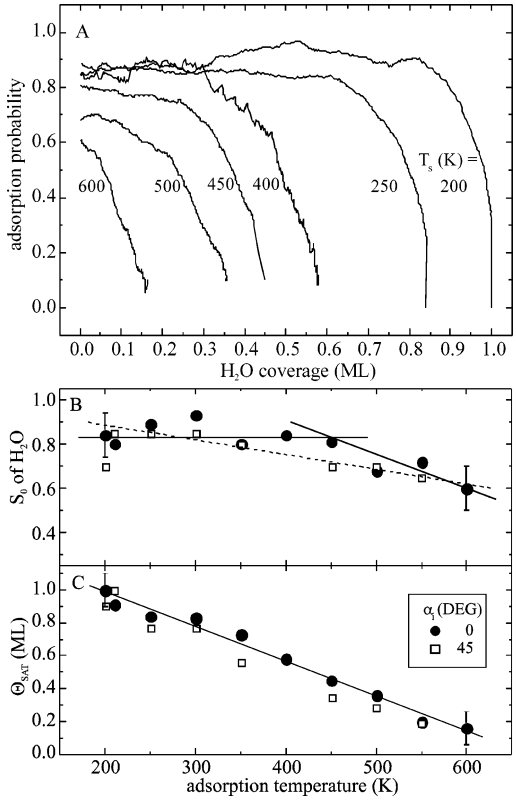

Figure 7. (A) $S(\Theta)$ of H_2O on O−ZnO parametric in T_s. (B) S_0 vs T_s, and (C) Θ_{Sat} vs T_s. (Solid spheres for $\alpha_i = 0°$, and open squares for $\alpha_i = 45°$).

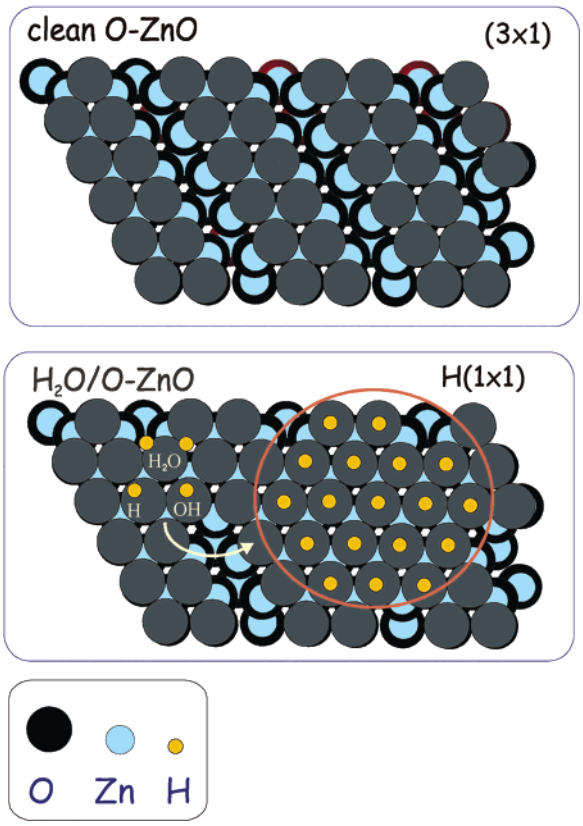

Figure 8. Structural models for (A) the clean O−ZnO surface characterized by an ordered (1 × 3) oxygen vacancy structure and **(**B) the H(1 × 1) O−ZnO surface.

both a displacive reconstruction, where the number of atoms in the unit cell is conserved but where individual atoms are displaced in a periodic fashion as well as the formation of an ordered array of vacancies (or adatoms) are possible. To obtain information on the stoichiometry of the surface which would help to distinguish between these different possibilities, we have carefully analyzed the XPS-data (using grazing exit angles of the photoelectrons in order to enhance the surface sensitivity) for the reconstructed surface.

The O 1s XPS-data reveal a main XP line at 531.6 eV with a weak shoulder at higher binding energy of 533.5 eV (see Figure 4A). Exposure of the sample to H_2O at a substrate temperature of 200 K leads to a significant increase in the intensity of the shoulder (a fitting procedure yields an increase of 40% for the data shown in Figure 4) associated with an increase of the total (integrated) O 1s intensity by 6 ± 1%. The surface structure resulting from H_2O-exposure is indistinguishable (He atom angular distributions and XPS-data) from the H(1 × 1)O−ZnO surface prepared by exposing the clean surface to hydrogen atoms. The quantitative analysis of the XPS-data thus strongly suggests that the clean (1 × 3)-structure exhibits a deficiency of O-atoms. The amount of missing O-atoms can be calculated according to

$$\frac{I_{1\times3}(\mathrm{O\ 1s})}{I_{1\times1}(\mathrm{O\ 1s})} = \frac{c_O^{s,1\times3} + c_O \sum_{n=1}^{\infty} e^{-n\cdot d/\lambda\cdot\cos\alpha}}{c_O + c_O \sum_{n=1}^{\infty} e^{-n\cdot d/\lambda\cdot\cos\alpha}} \qquad (1)$$

from the ratio of the total O 1s intensity before H_2O exposure, $I_{1\times3}$(O 1s), and after H_2O exposure, $I_{1\times1}$(O 1s). $c_O^{s,1\times3}$ and c_O are the oxygen concentrations in the top double layer (thickness *d*) of the O−ZnO(1 × 3) surface and of a stoichiometric ZnO double layer, respectively. When determining $I_{1\times3}$(O 1s) only the intensity in the XPS-data at 531.6 eV is considered, i.e., the shoulder at 533.7 eV seen for the (1 × 3) O−ZnO-surface (see Figure 4) is attributed to a small amount of OH-species already present at the surface before water adsorption. α denotes the exit angle of the photoelectrons with respect to the surface normal, and λ represents the mean free path of the photoelectrons. The XP peak intensities have been determined by fitting the spectra (see Figure 4A) with Gaussian line profiles after subtraction of a linear background. The photoelectron mean free path, λ, has not yet been determined experimentally for ZnO. Therefore we estimate λ by means of the TPP-2 formula (see ref 41), yielding $\lambda = 1.91$ nm for an electron kinetic energy of 956 eV with an estimated uncertainty of 10%. Accordingly, the estimated oxygen deficiency, Θ_{OV}, of the (1 × 3) top surface layer amounts to $\Theta_{OV} = 39 \pm 10\%$. The simplest arrangement consistent with an (1 × 3)-overlayer and a rather small oxygen deficit would be a unit-cell with one oxygen atom missing, as schematically depicted in Figure 8A. Such a model would lead to an oxygen deficit of 33% in the top plane, in good agreement with the experimental data. Further support for the presence of O-vacancies comes from CO adsorption measurements which have recently been conducted on the (1 × 3) O−ZnO surface (see ref 42). It has been shown theoretically that on a hypothetical (1 × 1) O−ZnO surface CO does not adsorb at temperatures above ∼30 K. The experimental finding that CO does indeed adsorb on this surface at temperatures below 80 K strongly suggests the presence of O-vacancies which allow a binding of CO to Zn-atoms as confirmed by theory.[42]

We therefore conclude that a (1 × 3)-unit cell with one O-atom vacancy is the simplest structure for the clean,

reconstructed (1 × 3) O−ZnO surface, consistent with the presently available experimental data.

(b) Adsorption of H_2O on the (1 × 3) O−ZnO Surface. Considering the fact that adsorption of water on the clean (1 × 3) O−ZnO surface is observed at temperatures above 200 K, associative adsorption of H_2O can be ruled out and strongly points toward a dissociative process. Since the resulting surface structure is indistinguishable from the H(1 × 1) O−ZnO surface as prepared by exposure to atomic hydrogen (same He atom angular distributions and an identical, distinct shoulder in the O 1s XP spectra), we conclude that H_2O is dissociated upon interaction with the surface, forming two OH-species per dissociated H_2O molecule.

The adsorption probability of H_2O on the O−ZnO surface for small coverages as determined by the King and Wells method amounts to ∼0.8 and remains approximately constant (see Figure 6) up to saturation of the surface. This kind of curve shape (Kisliuk-like shape, see refs 43, 44) strongly indicates that incident particles are first trapped in a precursor state. According to the Kisliuk-model, the particles trapped in the precursor state subsequently diffuse along the surface until adsorption of the species on a reactive surface site takes place. As a result, the adsorption probability becomes independent of the surface coverage, as observed in the experiment. By contrast, an adsorption scenario which would be dominated by direct adsorption events, i.e., an impact-induced dissociation without the influence of any precursor state, would lead to a linear decrease in $S(\Theta)$ with Θ according to Langmuirian adsorption dynamics. (The different possible adsorption scenarios are discussed in detail, e.g., in ref 45).

The initial adsorption probability, S_0, is found to be independent of the impact angle within the experimental uncertainty [±0.1], i.e., total energy scaling is obeyed as expected for a rather rough surface (see Figure 7C).

We therefore propose the following scenario for the adsorption of water on this surface: trapping of H_2O molecules in a precursor state, diffusion to an oxygen vacancy site, dissociation at the O-vacancy, formation of two OH-species, and finally the formation of (1 × 1) hydrogen islands (precursor-mediated dissociation, see Figure 8B).

Note, that a very similar scenario for water adsorption and dissociation has recently been observed for water adsorption on TiO_2 by Schaub et al.[25] In that study, the dissociation of H_2O on oxygen vacancy sites resulting in the formation of two OH-species could be directly observed in the STM. The main difference between the scenario proposed in the STM study and the present investigation is that an ordered O-vacancy structure has been observed for the O−ZnO surface whereas the oxygen vacancy sites are randomly distributed on TiO_2(110).

The decrease of the saturation coverage of H_2O with surface temperature (Figure 7C) is attributed to thermal desorption of water by recombination of H-atoms with OH-species, which is consistent with the He-TDS data shown in Figure 5. The decreases in S_0 with increasing T_s (Figure 7B) as well as the variation in the shape of $S(\Theta)$ above 500 K is also caused by thermal desorption of H_2O which leads to the detection of effective or kinetic adsorption probabilities in contrast to the measurements below ∼500 K, where dynamic adsorption probabilities are obtained (see, e.g., refs 45, 46).

(c) Adsorption of Water on the H(1 × 1) O−ZnO Surface. The observation of a dissociative adsorption of water on the O−ZnO surface is at variance with earlier TDS measurements by Zwicker and Jacobi[22] as well as Zhang et al.[23] Although we are unable to unambiguously explain these differences, we propose that in these previous experiments H_2O was adsorbed on an already hydrogenated surface. In our studies the desorption temperature of H_2O from H(1 × 1) O−ZnO (see below) was found to amount to 193 K which is in perfect agreement with the results of the previous TDS studies and supports our explanation. In our work the adsorption of water on the hydroxylated H(1 × 1) O−ZnO surface did not lead to the formation of ordered structures. Instead, the angular scans recorded for such physisorbed water adlayers (see Figure 1B) show a (1 × 1) structure superimposed on a broad cosine-shaped background, indicative of the formation of amorphous multilayers. A similar behavior has been reported in the previous work.[22]

(d) Determination of Kinetic Parameters for H_2O Interacting with the H(1 × 1) O−ZnO Surface. An independent way to monitor adsorption and desorption of water on the surface is to monitor the reflectivity of the specular He beam. The first derivative of I_{He} vs T_s curves can be compared to standard TDS curves (see, e.g., refs 40, 47 and the inset of Figure 5). In accord with the TDS data of refs 22 and 23, the low-temperature structure at 193 K in Figure 5 can be assigned to desorption of intact H_2O molecules weakly bound (physisorbed) to the OH-terminated H(1 × 1) O−ZnO surface. The broader structure observed at higher temperatures is assigned to either recombinative desorption of OH- and H-species (i.e., to the desorption of water) or to recombinative desorption of hydrogen atoms. After heating to 600 K, in all cases diffraction patterns typical for the (1 × 3) structure of the clean surface could be detected in the He atom angular distributions and the XPS-data reveal a O 1s line with no or a very small shoulder only.

Assuming a preexponential factor of 1×10^{21} mol^{-1} cm^2 s^{-1} [10,48] for recombinative desorption of hydrogen (at 500 K) leads to an activation energy for desorption (which here is assumed to be equal to the binding energy) of 130 kJ/mol (heating rate 1 K s^{-1}). This value compares well with the binding energy obtained before (137 kJ/mol) by He-TDS measurements after saturating a Zn−ZnO surface with atomic hydrogen, see ref 10. Note, however, that the structure in the He-TDS curve above 200 K is rather broad. This is certainly a clear indication that either more than one reaction pathway is involved in the H_2O desorption process or strong lateral interactions of the adsorbates might exist. Both mechanisms would explain the extended structure detected in the He-TDS curves. The binding energy given above should therefore be regarded as a rough estimate.

For the molecular desorption of H_2O from the H(1 × 1) O−ZnO surface, the binding energy (which again is assumed to be equal to the activation energy for desorption) can be obtained from the He-TDS peak at 193 K and is found to amount to 53 kJ/mol if a standard preexponential factor of 1×10^{13} s^{-1} is assumed.

6. Conclusions

According to recently published new results, the clean and hydrogen-free, ordered O−ZnO surface exhibits a (1 × 3) structure.[35] In these investigations the observation of large, ordered areas with a (1 × 1)-structure could be assigned to the presence of a hydrogenated (OH-terminated) surface. The H(1 × 1) surface can either be formed by exposing the reconstructed (1 × 3) O−ZnO surface to atomic hydrogen (see refs 35, 42) or to H_2O as shown in the present study. The XPS-data for the reconstructed, clean surface strongly indicate a deficit of surface oxygen with respect to a stoichiometric

O−ZnO surface. Since the high reactivity of the surface toward water indicates the presence of a large number of O-atoms vacancies, we propose that the (1 × 3) O−ZnO surface exhibits a unit-cell where one O-atom is missing.

The results obtained here for the adsorption probability of water on the clean O−ZnO surface clearly point toward the existence of a precursor state into which the H_2O molecules are trapped before dissociation. When in the course of their diffusive motion along the surface the H_2O molecules reach an O-vacancy, they can dissociate, yielding two OH-species on the surface. According to this model, one would in principle expect the presence of a (1 × 3)-structure also after H_2O adsorption, with a unit-cell containing two OH-species and one O-atom. Such a structure was never observed—neither after H_2O adsorption nor after exposure to atomic hydrogen. We thus propose that H-atoms adsorbed on the surface are rather mobile and diffuse to form well-ordered, fully hydroxylated H(1 × 1) islands. At present we cannot rule out that this process also leads to the formation of hydrogen-free patches exhibiting a (1 × 1) structure, see discussion above.

Note, that according to recent calculations the electrostatic instability of the clean (1 × 1) O−ZnO surface[42] is not removed upon adsorption of atomic H, i.e., the H(1 × 1) O−ZnO surface is also predicted theoretically to be unstable.[32,49] Also the (1 × 3)-structure of the reconstructed, clean surface has not yet been shown to be stable in theoretical calculations.[49] We speculate that both the (1 × 3)-structure observed for the clean surface and the H(1 × 1)-structure of the hydroxylated surface may be stabilized by the defect or step-edge stabilization mechanism proposed recently for the polar, Zn-terminated Zn−ZnO surface by Dulub et al.[32]

7. Summary

Structural as well as kinetic data characterizing the adsorption of H_2O on O−ZnO have been presented. Upon H_2O adsorption on the clean, reconstructed (1 × 3) O−ZnO surface an OH-terminated surface with a (1 × 1) structure is formed which is indistinguishable from the H(1 × 1) O−ZnO surface formed after exposing the clean (1 × 3) O−ZnO surface to atomic hydrogen.[35] The binding energy of the OH-species amounts to 130 kJ/mol (assuming a preexponential factor of 10^{21} mol^{-1} cm^2 s^{-1}) and the initial adsorption probability of water at thermal impact energies and at 250 K is $S_0 = 0.8 \pm 0.1$. The dissociation of the water molecules is proposed to take place at the O-vacancies of the clean, reconstructed (1 × 3) O−ZnO surface. The binding energy of water on the hydroxylated H(1 × 1)-surface is considerably smaller and amounts to 53 kJ/mol (assuming a preexponential factor of 10^{13} s^{-1}).

References and Notes

(1) Lopez, M. F.; Gutierrez, A.; Jimenez, J. A. *Surf. Sci*. **2001**, *482−485*, 300.
(2) Diebold, U. *Surf. Sci. Rep.* **2003**, *48*, 53.
(3) Henrich, V. E.; Cox, P. A. *The Surface Science of Metal Oxides*; Cambridge University Press: New York, 1996.
(4) Noguera, C. *Physics and Chemistry at Oxide Surfaces*; Cambridge University Press : New York, 1996.
(5) Freund, H. J.; Kuhlenbeck, H.; Staemmler, V. *Rep. Prog. Phys.* **1996**, *59*, 283.
(6) Askgaard, T. S.; Norskov, J. K.; Ovesen, C. V.; Stoltze, P. *J. Catal.* **1995**, *156*, 229.
(7) Hansen, J. B. Handbook of Heterogeneous Catalysis; Ertl, G., Knözinger, H., Weitkamp, J., Eds.; Wiley-VCH: Weinheim, 1997.
(8) Becker, T.; Kunat, M.; Boas, C.; Burghaus, U.; Wöll, C. *J. Chem. Phys.* **2000**, *113*, 6334.
(9) Becker, T.; Hövel, S.; Boas, C.; Kunat, M.; Burghaus, U.; Wöll, C. *Surf. Sci.* **2001**, *L502*.
(10) Becker, T.; Hövel, S.; Kunat, M.; Boas, C.; Burghaus, U.; Wöll, C. *Surf. Sci.* **2002**, *511*, 463.
(11) Becker, T.; Birkner, A.; Witte, G.; Wöll, C. *Phys. Rev. B* **2002**, *65*, 115401.
(12) Kunat, M.; Burghaus, U. JVST A **2003**, *21*, 1322.
(13) Stephan, J.; Burghaus, U. *Surf. Sci.* **2002**, *507−510*, 736.
(14) Thiel, P. A.; Madey, T. E. *Surf. Sci. Rep.* **1987**, *7*, 211.
(15) Sekine, R.; Adachi, H.; Morimoto, T. *Surf. Sci.* **1989**, *208*.
(16) Rodriguez, J. A.; Campbell, C. T. *Surf. Sci.* **1988**, *197*, 567.
(17) Casarin, M.; Maccato, C.; Vittadini, A. *Surf. Sci.* **1997**, *377−379*, 587.
(18) Sengupta, G.; Ahluwalia, H. S.; Banerjee, S.; Sen, S. P. *J. of Colloid Int. Sci.* **1979**, *69*, 217.
(19) Yasumoto, I. J. *Phys. Chem.* **1984**, *88*, 4041.
(20) Martins, J. B. L.; Andres, J.; Longo, E.; Taft, C. A. *Int. J. Quantum Chem.* **1996**, *57*, 861.
(21) Wander, A.; Harrison, N. M. *J. Chem. Phys.* **2001**, *115*, 2312.
(22) Zwicker, G.; Jacobi, K. *Surf. Sci.* **1983**, *131*, 179.
(23) Zhang, R.; Ludviksson, A.; Campbell, C. *Surf. Sci.* **1993**, *289*, 1.
(24) Hass, K. C.; Schneider, W. F.; Curioni, A.; Andreoni, W. *Science* **1998**, *282*, 265.
(25) Schaub, R.; Thostrup, P.; Lopez, N.; Laegsgaard, E.; Stensgaard, I.; Norskov, K. K.; Besenbacher, F. *Phys. Rev. Lett.* **2001**, *87*, 266104.
(26) Brinkley, D.; Dietrich, M.; Engel, T.; Farrall, P.; Gantner, G.; Schafer, A.; Szuchmacher, A. **1998**, *395*, 292.
(27) Wu, M. C.; Estrada, C. A.; Goodman, D. W. *Phys. Rev. Lett.* **1991**, *67*, 2910.
(28) Kim, Y. D.; Lynden-Bell, R. M.; Alavi, A.; Stulz, J.; Goodman, D. W. *Chem. Phys. Lett.* **2002**, *352*, 318.
(29) Schulze, M.; Reissner, R. *Surf. Sci.* **2001**, *482−485*, 285.
(30) Wander, A.; Schedin, F.; Steadmann, P.; Norris, A.; McGrath, R.; Turner, T. S.; Thornton, G.; Harrison, N. M. *Phys. Rev. Lett.* **2001**, *86*, 3811.
(31) Meyer, B.; Marx, D. *Phys. Rev. B* **2003**, *67*, 035403.
(32) Dulub, O.; Diebold, U.; Kresse, G. *Phys. Rev. Lett.* **2003**, *90*, 016102.
(33) Dulub, O.; Boatner, L. A.; Diebold, U. *Surf. Sci.* **2002**, *504*, 271.
(34) Brookes, I. M.; Muryn, C. A.; Thornton, G. *Phys. Rev. Lett.* **2001**, *87*, 266103.
(35) Kunat, M.; Gil-Girol, S.; Becker, T.; Burghaus, U.; Wöll, C. *Phys. Rev. B* **2002**, *66*, 081402(R).
(36) Hinch, B. J.; Lock, A.; Madden, H. H.; Toennies, J. P.; Witte, G. *Phys. Rev. B* **1990**, *42*, 1547.
(37) King, D. A.; Wells, M. G. *Surf. Sci.* **1972**, *29*, 454.
(38) Xu, C.; Koel, B. E.; Paffett, M. T. *Langmuir* **1994**, *10*, 166.
(39) Scoles, G. Atomic and Molecular Beam Methods; Scoles, G., Ed.; Oxford University Press, New York, 1988.
(40) Libuda, J.; Scoles, G. J. *Chem. Phys.* **2000**, *112*, 1522.
(41) Tanuma, S.; Powell, C. J.; Penn, D. R. *Interface Anal.* **1993**, *20*, 77.
(42) Staemmler, V.; Fink, K.; Meyer, B.; Marx, D.; Kunat, M.; Burghaus, U.; Gil-Girol, S.; Wöll, C. *Phys. Rev. Lett.* **2003**, *90*, 106102-1.
(43) Kisliuk, P. *J. Phys. Chem. Solids* **1958**, *5*, 78.
(44) Kisliuk, P. *J. Phys. Chem. Solids* **1957**, *3*, 95.
(45) Burghaus, U. *Trends Phys. Chem.* **2001**, *8*, 21.
(46) Ding, J.; Burghaus, U.; Weinberg, W. H. *Surf. Sci.* **2000**, *446*, 46.
(47) Canepa, M.; Terreni, S.; Narducci, E.; Mattera, L. *J. of Chem. Phys.* **1999**, *110*, 2257.
(48) Waugh, K. C. *Catal. Today* **1999**, *53*, 161.
(49) Meyer, B. Submitted for publication.